Allosteric Binding Properties of a Monoclonal Antibody and Its Fab Fragment†

Robert C. Blake II,[‡,§] James B. Delehanty,[⊥,||] Mehraban Khosraviani,[⊥,#] Haini Yu,[⊥] R. Mark Jones,[⊥,¶] and Diane A. Blake*[,⊥,§]

Department of Ophthalmology, Tulane University Health Sciences Center, 1430 Tulane Avenue, New Orleans, Louisiana 70112, College of Pharmacy, Xavier University of Louisiana, New Orleans, Louisiana 70125, and Tulane/Xavier Center for Bioenvironmental Research, New Orleans, Louisiana 70112

Received August 27, 2002; Revised Manuscript Received October 19, 2002

ABSTRACT: Detailed equilibrium binding studies were conducted on a monoclonal antibody directed against Pb(II) complexed with a protein conjugate of diethylenetriaminepentaacetic acid (DTPA). Binding curves obtained with DTPA and a cyclohexyl derivative of DTPA in the presence and absence of metal ions were consistent with the anticipated one-site homogeneous binding model. Binding curves obtained with aminobenzyl−DTPA or its complexes with Ca(II), Sr(II), and Ba(II) were highly sigmoidal, characterized by Hill coefficients of 2.3−6.5. Binding curves obtained with the Pb(II) and In(III) complexes of aminobenzyl−DTPA were hyperbolic, but in each case the apparent affinity of the antibody for the chelator−metal complex was higher in the presence of excess chelator than it was in the presence of excess metal ion. In the presence of excess chelator, the equilibrium dissociation constant for the binding of aminobenzyl−DTPA−Pb(II) to the antibody was 9.5×10^{-10} M. Binding curves obtained with the Hg(II) and Cd(II) complexes of aminobenzyl−DTPA were biphasic, indicative of negative cooperativity. Further binding studies demonstrated that aminobenzyl−DTPA−Hg(II) opposed the binding of additional chelator−metal complexes to the antibody more strongly than did aminobenzyl−DTPA−Cd(II). The Fab fragment differed from the intact antibody only in that the apparent affinity of the Fab was generally lower for a given chelator−metal complex. These data are interpreted in terms of a model in which (i) aminobenzyl−DTPA and its complexes bind both to the antigen binding site and to multiple charged sites on the surface of the compact immunoglobulin; and (ii) the bound, highly charged ligands interact in a complicated fashion through the apolar core of the folded antibody.

It is generally accepted that the binding of small antigens to bivalent antibodies proceeds as though the two antigen binding sites were equal and functionally independent. Indeed, a search conducted in the vast literature on this subject over the last 40 years reveals only one clear exception to this generalization (*1*). Polyclonal antisera produced by rabbits immunized with protein conjugates of either L-thyroxine or 3,5,3′-triiodo-L-thyronine were reported to bind the corresponding soluble antigens with a high degree of positive cooperativity. In contrast to the scarcity of literature on allosteric effects due to antigen binding-dependent conformation changes in the antibody, many laboratories have reported that protein antigens can display positive cooperativity in the binding of multiple antibodies to different epitopes on the antigen (*2*−*13*). In each of these latter examples, however, the positive cooperativity was thought to arise either from conformation changes in the protein antigen that occurred as a consequence of antibody binding (*2*−*6*), or from cyclic structures that could form as a consequence of the multivalency of both the antibody and the protein antigen (*7*−*13*). In either case, binding-induced conformation changes in the antibodies were neither postulated nor required to rationalize the experimental observations.

As part of an ongoing effort in our laboratories to develop immunoassays for heavy metals and other environmental contaminants, we have produced and characterized a growing number of monoclonal antibodies directed toward epitopes of metal−chelator complexes (*14*−*17*). One such antibody, designated as 2C12, was reported to bind the 1:1 complex of cyclohexyldiethylenetriamine pentaacetic acid (CHX−DTPA)[1] and Pb(II) with positive cooperativity (Hill coefficient of 2.1) when the metal−chelator complex was diluted from a concentrated stock solution (*15*). Control experiments showed that (i) only the CHX−DTPA−Pb(II) complex bound with high affinity to 2C12 and (ii) dissociation of the Pb(II) from the CHX−DTPA−Pb(II) complex occurred over

† This research was supported by the Office of Science (BER), U.S. Department of Energy, Grant No. DE-FG02-98ER62704 and by Grant No. 82799(3CEN), U.S. Department of Energy EMSP (D.A.B.). Additional support was provided by grants to R.C.B.II from the National Institutes of Environmental Health Sciences ARCH Program (5 S11 ES09996−03) and the National Institutes of Health (GM08008−26S1). J.B.D. was supported in part by a scholarship from the Tulane/Xavier Center for Bioenvironmental Research.

* To whom correspondence should be addressed at Tulane University Health Sciences Center. Phone: (504) 584-2478. Fax (504) 584-2684. E-mail: blake@tulane.edu.

‡ Xavier University of Louisiana.

§ Tulane/Xavier Center for Bioenvironmental Research.

⊥ Tulane University Health Sciences Center.

|| Present address: Naval Research Laboratory, 4555 Overlook Ave, SW, Washington, DC 20375.

Present address: LINCO Research, Inc., 14 Research Park Drive, St. Charles, MO 63304.

¶ Present address: Sapidyne Instruments, Inc., 967 E. Park Center Blvd., Boise, ID 83706.

10.1021/bi0267339 CCC: $25.00
Published on Web 12/19/2002

the same concentration range as that employed in the antibody binding study. Thus, the apparent positive cooperativity was attributed to the bimolecular association of equal concentrations of the CHX−DTPA and the Pb(II) to form the complex actually recognized by the antibody, not to some binding-dependent conformation change in the antibody.

The present study describes the extraordinary binding properties of a monoclonal antibody directed against an epitope comprised of Pb(II) complexed with a protein conjugate of thioureido-L-benzyl−DTPA. In contrast to 2C12, this new antibody exhibited a remarkable range of allosteric binding reactions when the antibody was presented with selected chelators, metal−chelator complexes, or various combinations of the two. Under appropriate solution conditions, this antibody exhibited normal homogeneous binding, homotropic positive cooperativity, heterotropic positive cooperativity, homotropic negative cooperativity, and heterotropic negative cooperativity. The same range of allosteric binding behavior was also observed with the corresponding Fab fragment prepared by proteolytic cleavage of the antibody. Care was taken in the present study to avoid chelator and metal ion concentrations that would permit significant dissociation of the metal−chelate complex in the concentration range used in each binding experiment. This practice ensured that the two principal small ligand species in each binding mixture were the chelator−metal complex and an excess of either the metal-free chelator or the chelator-free metal ion. Where appropriate, control experiments indicated that equivalent concentrations of the chelator or the metal ion in excess exhibited little or no direct binding to the antigen binding site on the antibody. Therefore, the remarkable binding properties described herein are attributed to the antibody itself and are hypothesized to arise from interactions among charged ligands that bind to multiple sites on the Fab portion of the immunoglobulin.

EXPERIMENTAL PROCEDURES

Materials. BALB/c inbred mice were purchased from Charles River Laboratories (Wilmington, MA). SP2/0-Ag14 myeloma cells were from the American Type Tissue Collection (Rockville, MD). Ultrapure bovine serum albumin (BSA) and the IsoStrip mouse monoclonal antibody isotyping kit were from Boehringer-Mannheim Biochemicals (Indianapolis, IN). Keyhole limpet hemocyanin was purchased from Calbiochem (La Jolla, CA). 1B4M−DTPA and CHX−DTPA were available from previous studies (*15*). *p*-Aminobenzyl−DTPA was a product of Macrocylics, Inc. (Dallas, TX). Atomic absorption grade metals were purchased from Perkin-Elmer Corp. (Norwalk, CT). DTPA, HEPES buffer, tissue culture medium, pristane, Tween-20, trinitrobenzenesulfonic acid, L-glutamine, antibiotics, and goat anti-mouse IgG conjugated to horseradish peroxidase were obtained from Sigma Chemical Co. (St. Louis, MO). Fetal bovine serum was a product of HyClone Laboratries (Logan, UT). Reagents for monoclonal antibody production were included in the ClonaCell-HY monoclonal antibody production kit (StemCell Technologies, Vancouver, BC, Canada). Microwell plates for ELISA (flat-bottom, high-binding) and tissue culture plates were purchased from Corning Costar (Cambridge, MA). 3,3′,5,5′-Tetramethylbenzidine peroxidase substrate (TMB Microwell Substrate) was from Kirkegaard-Perry Laboratories (Gaithersburg, MD). The Fab preparation kit and BCA protein assay kit were purchased from Pierce Chemical Co. (Rockford, IL) and used according to manufacturer's protocols. Poly-(methyl methacrylate) beads (98 ± 8 μm diameter) were provided by Sapidyne Instruments (Boise, ID). The Cy5 conjugates of affinity-purified goat anti-mouse Fc-specific and F(ab)′$_2$-specific antibodies were purchased from Jackson ImmunoResearch Laboratories (West Grove, PA). All other materials were obtained as noted in the text.

Preparation of Protein−Chelate Conjugates. Protein−chelate conjugates were prepared by a modification of a previously described method (*15*, *18*) in a final volume of 1 mL containing 10 mg of protein (BSA or KLH), 1.7 mM 1B4M-DTPA, 2.0 mM $Pb(NO_3)_2$, and 47 mM triethylamine in 100 mM HEPES buffer (pH 9.5). The reactions were stirred for 24 h at 25 °C. A metal-free BSA conjugate was prepared by omitting the $Pb(NO_3)_2$ from the reaction mixture. Unreacted low-molecular weight reactants were removed by buffer exchange using a Centricon-30 concentrator device (Amicon, Beverly, MA). The protein conjugates were characterized using the trinitrobenzenesulfonic acid method described in ref 19. The extent of substitution of free lysine residues was 21.1% for the BSA conjugate and 46.2% for the KLH conjugate.

Mouse Immunization, Hybridoma Production, and Monoclonal Antibody Purification. Three 6−7-week-old female BALB/c mice were injected in both the neck and the base of the tail with a total of 250 μg of the KLH conjugate emulsified in Ribi adjuvant (Ribi Immunochemicals, Hamilton, MT) at days 0, 21, and then at 2-week intervals. The antibody response of each mouse was determined by indirect ELISA as described in ref 20 using both metal-free BSA−benzyl−DTPA and the conjugate complexed with Pb(II). The mouse with the highest antibody response was given a final intravenous tail vein boost with 200 μg of the KLH conjugate in phosphate-buffered saline (PBS, 137 mM NaCl, 3 mM KCl, 10 mM sodium phosphate buffer, pH 7.4) 72 h prior to sacrifice. Mouse spleen cells were harvested, washed twice in RPMI 1640 medium, and fused with SP2/0-Ag14 myeloma cells. Fused cells were grown in semisolid medium selective for the growth of hybridoma clones according to the protocol included in the ClonaCell-HY kit. Individual clones were transferred to separate wells of 96-well tissue culture plates and incubated at 37 °C in a humidified atmosphere supplemented with 5% CO_2. Supernatants from replicating hybridomas were collected and screened for antibodies to DTPA−Pb(II) by competitive inhibition ELISA

[1] Abbreviations: CHX-DTPA, *trans*-cyclohexyldiethylenetriamine-*N*,*N*′,*N*′,*N*″,*N*″-pentaacetic acid; DTPA, diethylenetriamine-*N*,*N*′,*N*′,*N*″,*N*″-pentaacetic acid; aminobenzyl-DTPA; *p*-aminobenzyldiethylenetriamine-*N*,*N*′,*N*′,*N*″,*N*″-pentaacetic acid; BSA, bovine serum albumin; BSA-benzyl-DTPA-Pb(II); bovine serum albumin-thioureido-L-benzyl-diethylenetriamine-*N*,*N*′,*N*′,*N*″,*N*″-pentaacetic acid-Pb(II) covalent conjugate; KLH, keyhole limpet hemocyanin; ELISA, enzyme-linked immunosorbent assay; Fab, fragment antigen binding (monovalent); F(ab)′$_2$, fragment antigen binding (bivalent); Fc, fragment crystallizable; HEPES, (*N*-[2-hydroxyethyl]piperazine-*N*′-[2-ethanesulfonic acid]); HBS, HEPES buffered saline; SDS−PAGE, sodium dodecyl sulfate−polyacrylamide gel electrophoresis; DEAE-cellulose, diethylaminoethyl cellulose; V_H, heavy chain variable region; V_L, light chain variable region; C_H, heavy chain constant domain; C_L, light chain constant domain.

as described in ref 20. Positive hybridoma clones were subcultured and frozen.

Ascites fluid was produced in pristine-primed BALB/c mice by intraperitoneal injection of 1.6×10^6 hybridoma cells (clone designation 5B2). Ascites fluid was collected 7−10 days after hybridoma injection, and the IgG fraction of ascites was isolated by ammonium sulfate precipitation followed by ion-exchange chromatography using DEAE-cellulose (DE−52, Whatman, Inc., Clifton, NJ) (*21*). SDS−PAGE of the purified protein showed bands for only heavy and light chains (data not shown). The protein concentration of the purified antibody was determined using the BCA protein assay kit. The immunoglobulin subclass of the 5B2 monoclonal antibody was determined and quantified by sandwich ELISA using antibodies specific for IgG1, IgG2a, IgG2b, IgG3, IgM, and IgA and the light chain was isotyped using the IsoStrip antibody isotyping kit according to the manufacturer's protocol.

Competitive Inhibition ELISA. Competitive inhibition ELISAs were performed essentially as described in ref 20. Ag(I), Al(III), Ca(II), Cd(II), Co(II), Cu(II), Fe(III), Hg(II), In(III), Mg(II), Mn(II), Mo(VI), Ni(II), Pb(II), Sr(II), and Zn(II) were assayed for their ability to inhibit the purified 5B2 mAb from binding to the immobilized BSA−benzyl−DTPA−Pb(II) conjugate in a background of 0.7 mM DTPA.

Preparation and Characterization of Fab from 5B2. A monovalent Fab fragment of the 5B2 mAb was prepared using the Immunopure Fab Preparation kit (Pierce Chemical Co., Rockford, IL). The intact antibody was subjected to proteolysis with immobilized papain and the progress of the enzymatic digestion was monitored by SDS−PAGE followed by both Coomassie staining and Western blotting using Fc- and light chain-specific antibodies (data not shown). The Fc and undigested IgG fragments were removed by passing the digestion reaction over a column of immobilized protein A. The final yield of Fab was 19.0% of the initial IgG.

Calculation of Metal and Chelator Speciation. The concentrations of free and complexed metal ions and aminobenzyl−DTPA were estimated using the published values for the corresponding DTPA-metal ion formation constants (*22*) and assuming that aminobenzyl−DTPA behaved identically to DTPA with regard to its metal-binding properties. In studies with Y(III), the addition of a substituent to the backbone of the DTPA molecule increased the stability of the metal−chelate complex (*23*), so our assumption of identity is a conservative estimate. Published values for the standard formation constants for DTPA and individual metal ions were multiplied by 3.98×10^{-4} to convert the standard formation constants to conditional formation constants at pH 7.4 (*24*).

Determination of Equilibrium Binding Constants. Equilibrium measurements of the interactions of metal-free chelators and chelator−metal complexes with the intact 5B2 antibody and its Fab fragment were performed on a KinExA 3000 immunoassay instrument (Sapidyne Instruments, Inc., Boise, ID) (*25, 26*). The assay format was identical to that described previously (*15*) with the following two exceptions: (i) the immobilized capture reagent adsorption-coated onto the hydrophobic beads was BSA−benzyl−DTPA−Pb(II) rather than the corresponding CHX−DTPA protein-conjugate; and (ii) the anti-mouse secondary antibodies used to quantify the extent of binding of 5B2 and its Fab to the immobilized antigen were covalently labeled with the Cy5 fluorophore rather than Cy3. When the primary antibody was the Fab fragment, the bead reservoir on the instrument was amended with 1.0 μM $Pb(NO_3)_2$ to ensure that all of the chelator sites on the immobilized capture reagent were complexed with lead ions. In addition, BSA at a final concentration of 0.1% (w/v) was added to all equilibrium reactions that contained the Fab to stabilize the fragment.

Equilibrium measurements where the soluble chelator was DTPA or CHX−DTPA were conducted with 5B2 and Fab fragment concentrations of 0.2 and 1.0 μg/mL, respectively. The concentration of metal ion, when present, was always in excess to that of the chelator; the individual concentrations are given in the appropriate table legend. Equilibrium measurements with BSA−benzyl−DTPA−Pb(II) were conducted with 5B2 and Fab fragment concentrations of 40 and 50 ng/mL, respectively.

Equilibrium measurements where the soluble chelator was aminobenzyl−DTPA were also conducted with 5B2 and Fab fragment concentrations of 40 and 50 ng/mL, respectively. All measurements that involved aminobenzyl−DTPA−metal ion complexes were conducted in the presence of an excess concentration of either the chelator or the metal ion; the identity and concentration of the reagent present in excess are included in the legends to the appropriate tables. For all binding studies, data acquisition was achieved via a PC interfaced to the KinExA and software provided by Sapidyne Instruments, Inc. Equilibrium dissociation constants were determined from nonlinear regression analysis of the data using the equations described below and software contained in SlideWrite 5.0 (Advanced Graphics, Encinitas, CA).

N-Terminal Sequencing of Immunoglobulin Light and Heavy Chains. Prior to N-terminal sequencing, the DEAE-purified 5B2 mAb was further purified by affinity chromatography on immobilized BSA−benzyl−DTPA−Pb(II) conjugate. Because the yield of protein from this column was low, approximately 10%, equilibrium dissociation constants for several different metal−chelate ligands were determined for the recovered material and were identical to the starting material (data not shown). Immunoglobulin light and heavy chains were separated by 10% SDS−PAGE under reducing conditions and transferred to MiniProBlott membrane (Applied Biosystems, Inc., Foster City, CA). Samples were sequenced by Edman degradation in an institutional facility (Louisiana State University Health Sciences Center, New Orleans, LA) using a Procise 494 Protein Sequencer (Applied Biosystems, Inc.).

RESULTS

Design of Immunogen and Animal Response. The Pb(II)−chelate hapten described in these studies was not of adequate size to generate an immune response. Therefore, DTPA was covalently coupled to a carrier protein (KLH), loaded with Pb(II), and used as an immunogen. The KLH−benzyl−DTPA−Pb(II) conjugate was injected into BALB/c mice and the presence of antibodies that preferentially recognized the Pb(II)-loaded DTPA compared to the Pb(II)-free DTPA was assessed by indirect ELISA (data not shown). The mouse producing antibodies with the greatest differential binding activity was given a final tail vein injection of the KLH conjugate and spleen cells were harvested 72 h later for the preparation of hybridoma cells.

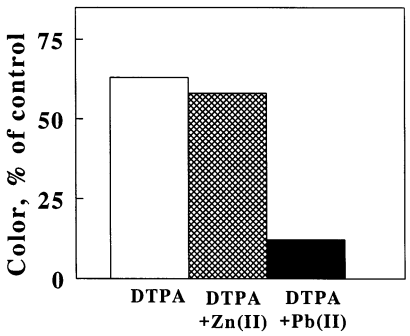

FIGURE 1: Screening of culture supernatants by competitive ELISA. Tissue culture supernatant from the 5B2 hybridoma was diluted in HBS and tested by competitive ELISA for its ability to be inhibited by the addition of 10 mM DTPA (open bars), 760 μM Zn(II) in 10 mM DTPA (gray bars), or 482 μM Pb(II) in 10 mM DTPA (black bars). Results are expressed as percent of control (HBS only).

Hybridoma Screening. Screening of 1440 hybridoma culture supernatants by indirect ELISA for their ability to bind immobilized BSA−benzyl−DTPA−Pb(II) identified 35 positive clones. These hybridomas were further analyzed by competitive inhibition ELISA to determine antibody specificity. The majority (*33*) of these 35 clones exhibited affinity for either the metal-free chelator or the benzyl isocyanato moiety that was part of the conjugated epitope. Only two clones produced antibodies whose binding was competitively inhibited by metal-laden DTPA but not metal-free DTPA. Cells from the single clone that appeared to recognize Pb(II)-loaded DTPA were subcloned by limiting dilution to give rise to the hybridoma 5B2. As illustrated in Figure 1, the antibody produced by this clone exhibited moderate inhibition by metal-free DTPA (10 mM) or DTPA−Zn(II) (37 and 42% inhibition, respectively). However, incubation of the antibody with DTPA−Pb(II) (482 μM Pb(II) in 10 mM DTPA) resulted in an 88% inhibition of binding activity. Ascites from this clone was produced and purified to obtain sufficient antibody for subsequent characterization. Isotyping revealed that the monoclonal antibody synthesized by the 5B2 hybridoma was of subclass IgG_1 with a λ light chain. Competitive inhibition ELISA with the DTPA complexes of 16 different metal ions indicated that only Pb(II) and In(III) had any significant inhibitory activity (data not shown).

Equilibrium Binding Studies. The affinity and specificity of antibody 5B2 for various combinations of chelators and metal ions were determined using a KinExA 3000 immunoassay instrument. Briefly, the KinExA is a flow fluorimeter that separates and quantifies the fraction of antibody binding sites that remain unoccupied in reaction mixtures of antibody, antigen, and antibody−antigen complexes (*14*, *15*, *25*, *26*). Polymer beads coated with immobilized antigen were deposited in the observation cell of the instrument and exploited to capture and retain those antibody molecules with unoccupied binding sites. The quantity of primary antibody thus captured was then determined by exposing the beads to a fluorescently labeled anti-mouse secondary antibody. The principal feature of KinExA assays is that the interaction to be quantified is that of the binding reactions in homogeneous solution; the immobilized antigen is simply a tool used to capture and quantify those antibodies with unoccupied binding sites in the solution mixture.

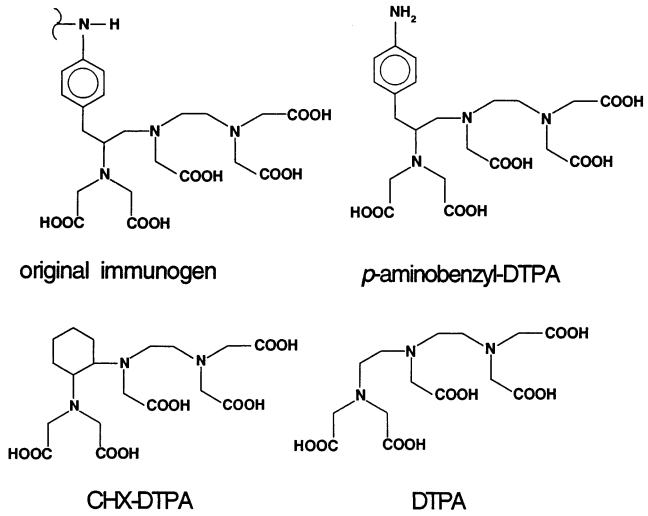

FIGURE 2: Structure of metal chelators. Shown are the structures of the metal-chelators used in this study. The original immunogen represents *p*-benzyl isothiocyano DTPA that was covalently coupled to keyhole limpet hemocyanin (KLH). *p*-Aminobenzyl−DTPA, CHX−DTPA, and DTPA are low molecular weight analogues of the immunogen.

Equilibrium binding studies were conducted with 5B2 and its Fab fragment using a variety of soluble chelators and metal ions; the structures of the chelators exploited herein are shown in Figure 2. The original immunogen was the thioureido conjugate formed when isothiocyanatobenzyl−DTPA was reacted with keyhole limpet hemocyanin. All of the equilibrium binding data fell into one of five categories: (i) homogeneous; (ii) homotropic positive; (iii) homotropic negative; (iv) heterotropic positive; and (v) heterotropic negative. Homogeneous binding curves were obtained when the chelator−metal complex exhibited no evidence for concentration-dependent changes in the apparent affinity of the protein for the complex. Homotropic positive or negative binding curves were obtained when increasing concentrations of a chelator−metal complex appeared to increase or decrease, respectively, the affinity of the remaining binding sites on the protein for the same complex. Heterotropic positive or negative binding curves were obtained when the presence of a particular chelator−metal complex appeared to increase or decrease, respectively, the affinity of the protein for a different chelator−metal complex.

Homogeneous Binding. When the chelator was soluble, unconjugated DTPA, equilibrium binding studies conducted on the KinExA produced binding curves that were consistent with the one-site, homogeneous binding model anticipated for an antibody−antigen interaction where the two sites on the bivalent antibody behave as though they are independent. Representative binding curves obtained with intact 5B2 are shown in Figure 3A. The low affinity curve in Figure 3A was obtained with metal-free DTPA, while the high affinity curve was obtained with the corresponding DTPA−Pb(II) complex. The value of the equilibrium dissociation constant, K_d, obtained from each curve in Figure 3A was determined from a nonlinear regression fit of the data to the following equation:

$$\text{fraction of occupied binding sites} = \frac{[L]}{K_d + [L]} \quad (1)$$

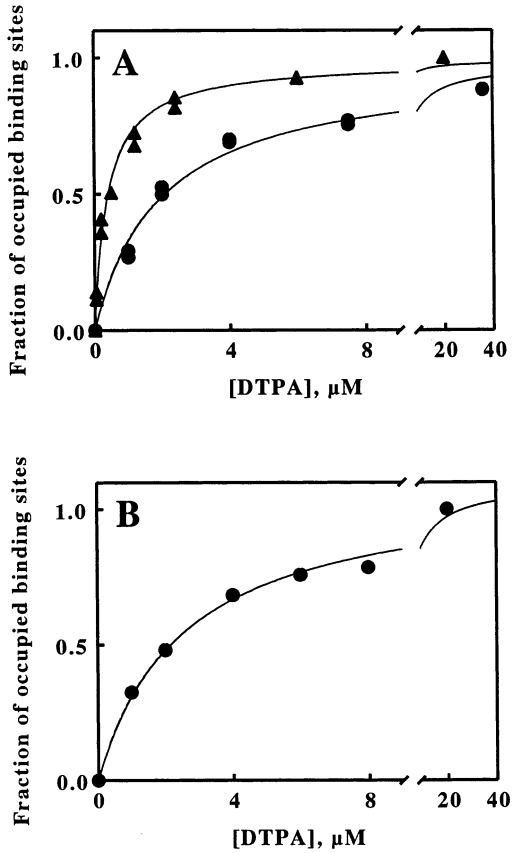

FIGURE 3: Homogeneous binding of chelator−metal ion complexes to intact 5B2 (A) and its Fab fragment (B). Panel A, concentration dependence of the binding of DTPA to intact 5B2 in the presence (triangles) and absence (circles) of 20 μM Pb(II). Panel B, concentration dependence of the binding of DTPA to the Fab of 5B2 in the presence of 20 μM Pb(II). Each determination was performed in duplicate. The hyperbolic curves drawn through the data points were generated using eq 1 in the text and the values for the corresponding equilibrium dissociation constants shown in Table 1.

where [L] is the concentration of soluble antigen. Values of 3.9×10^{-7} and 1.9×10^{-6} M were determined for the equilibrium dissociation constants for the binding of DTPA−Pb(II) and metal-free DTPA, respectively, with intact 5B2. Binding curves for the interaction of DTPA−Ca(II) and DTPA−Sr(II) with intact 5B2 were essentially indistinguishable from that obtained with the metal-free chelator (primary data not shown). The only other DTPA−metal ion complex that 5B2 appeared to bind more tightly than the metal-free chelator was the 1:1 complex formed between DTPA and In(III). The dissociation constant for the DTPA−In(III) complex was 5.6×10^{-7} M; thus, 5B2 binds to the DTPA−Pb(II) complex with an affinity only approximately 1.4 greater than that observed for the DTPA−In(III) complex. These binding data are summarized in Table 1.

Similar results were obtained when CHX−DTPA was substituted for DTPA (Table 1). Introduction of the more rigid cyclohexyl ring into the structure of DTPA lowered the affinity of intact 5B2 for the metal-free chelator by only 3-fold, but increased the affinity for the corresponding complex with Pb(II) by 2-fold. Once again, the affinities of intact 5B2 for the Ca(II) and Sr(II) complexes of CHX-DTPA were very close to that for the metal-free chelator.

Covalent conjugation of aminobenzyl−DTPA to bovine serum albumin by a thioureido linkage had a dramatic effect on the affinity of 5B2 for the Pb(II) complex with the chelator; the equilibrium dissociation constant for the binding of BSA−benzyl−DTPA−Pb(II) to the intact antibody was 1.4×10^{-9} M, a value 2 orders of magnitude lower than that obtained with the unconjugated DTPA−Pb(II) complex.

Table 1: Homogeneous Binding of Chelators and Metal−Chelate Complexes to Intact 5B2 and Its Fab Fragment

protein	chelator	metal ion	equilibrium dissociation constant[a] (M)
intact 5B2	DTPA	metal-free	$1.9 \pm 0.3 \times 10^{-6}$
		Pb(II)[b]	$3.9 \pm 0.7 \times 10^{-7}$
		Ca(II)[c]	$1.1 \pm 0.1 \times 10^{-6}$
		Sr(II)[d]	$1.6 \pm 0.3 \times 10^{-6}$
		In(III)[e]	$5.6 \pm 1.1 \times 10^{-7}$
	CHX−DTPA	metal-free	$6.1 \pm 1.4 \times 10^{-6}$
		Pb(II)[b]	$2.3 \pm 0.5 \times 10^{-7}$
		Ca(II)[c]	$3.9 \pm 0.4 \times 10^{-6}$
		Sr(II)[f]	$4.1 \pm 0.5 \times 10^{-6}$
	BSA−benzyl−DTPA	Pb(II)	$1.4 \pm 0.4 \times 10^{-9}$[g]
Fab of 5B2	DTPA	Pb(II)[b]	$2.6 \pm 0.7 \times 10^{-6}$
	CHX−DTPA	Pb(II)[b]	$2.0 \pm 0.3 \times 10^{-6}$
	BSA−benzyl−DTPA	Pb(II)	$5.9 \pm 1.0 \times 10^{-10}$[g]

[a] Equilibrium dissociation constants are shown with their 95% confidence intervals. The structures of the chelators are shown in Figure 2. [b] [Pb(II)] = 20 μM. [c] [Ca(II)] = 40 μM. [d] [Sr(II)] = 40 μM. [e] Equimolar concentrations of In(III) and DTPA up to 40 μM each. [f] [Sr(II)] = 125 μM. [g] Expressed as concentration of BSA.

The Fab fragment derived from the proteolytic cleavage of intact 5B2 exhibited a lower affinity for the soluble DTPA−Pb(II) complex than did the intact antibody. The binding curve shown in Figure 3B was obtained when the Fab of 5B2 was incubated with limiting concentrations of DTPA in the presence of 20 μM Pb(II). A nonlinear regression fit of the data in Figure 3B to eq 1 yielded an equilibrium dissociation constant for the binding of DTPA−Pb(II) to the Fab of 2.6×10^{-6} M, an affinity over 6-fold lower than that observed for the binding of the same complex to the intact 5B2. Similarly, the Fab bound the CHX−DTPA−Pb(II) complex with 10-fold lower affinity than did the intact antibody (Table 1). Surprisingly, the equilibrium dissociation constant for the binding of BSA−benzyl−DTPA−Pb(II) to the Fab was not similarly influenced ($K_d = 5.9 \times 10^{-10}$ M). Regardless of the identity of the chelator or the metal ion, all of the equilibrium dissociation constants given in Table 1 were obtained from hyperbolic binding curves that represented the single, one-site homogeneous binding model.

Homotropic Positive Cooperativity. When aminobenzyl−DTPA was substituted for DTPA or CHX−DTPA in equilibrium binding studies conducted on the KinExA, certain combinations of chelators and metal ions produced binding curves that indicated a high degree of homotropic positive cooperativity in the interaction of the metal−chelator complex with the antibody. The equilibrium binding data shown in Figure 4A were obtained when intact 5B2 was incubated with limiting concentrations of aminobenzyl−DTPA in the presence of 100 mM Ca(II). The excess concentration of Ca(II) ensured that the chelator would be present as the corresponding complex with Ca(II); control experiments demonstrated that 100 mM Ca(II) had no apparent effect on the interaction of the soluble 5B2 with the immobilized capture reagent used to quantify the extent

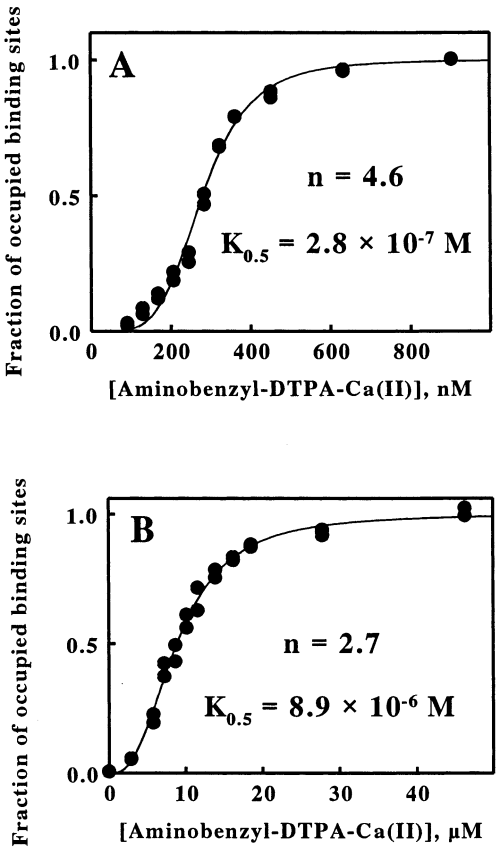

FIGURE 4: Homotropic positive cooperativity in the binding of aminobenzyl−DTPA−Ca(II) to intact 5B2 (A) and its Fab fragment (B). DTPA at the concentrations shown on the *x*-axis was varied while holding Ca(II) at 100 mM in all experiments. Each determination was performed in duplicate; in many cases the error in the data was less than the diameter of the plotted points. The data were fit to the Hill equation (eq 2 in the text) and parameters for the sigmoidal curves drawn through the data points were determined by nonlinear regression analyses. $K_{0.5}$ is the concentration of aminobenzyl−DTPA−Ca(II) that resulted in occupancy of half of the available antibody binding sites and *n* represents the Hill coefficient determined for each curve.

of binding in solution. The parameters for the sigmoidal curve drawn through the data points in Figure 4A were obtained from a nonlinear regression fit of the data to the following equation:

$$\text{fraction of occupied binding sites} = \frac{[\text{L}]^n}{[\text{L}]^n + [K_{0.5}]^n} \quad (2)$$

where *n* (the Hill coefficient) is a number greater than 1.0 and $K_{0.5}$ is the concentration of aminobenzyl−DTPA−Ca(II) that resulted in occupancy of half of the available antibody binding sites. Values of 2.8 × 10^{-7} M and 4.6 for $K_{0.5}$ and *n*, respectively, produced the best fit of the regression line to the data in Figure 4A.

Identical binding studies were conducted with the monovalent Fab fragment derived from proteolytic cleavage of the intact 5B2. The equilibrium binding data shown in Figure 4B were obtained when the Fab fragment of 5B2 was incubated with aminobenzyl−DTPA−Ca(II). As was the case with the intact antibody, control experiments showed that 100 mM Ca(II) did not influence binding and capture of the Fab fragment by the immobilized antigen. A nonlinear regression fit of these data to eq 2 yielded values for $K_{0.5}$ and *n* of 8.9 × 10^{-6} M and 4.5, respectively.

Table 2: Homotropic Positive Cooperativity in the Binding of Aminobenzyl−DTPA and Its Alkaline Earth Complexes to Intact 5B2 and Its Fab Fragment

protein	aminobenzyl−DTPA complex	$K_{0.5}$, M[a]	Hill coefficient[a]
intact 5B2	metal-free	3.2 ± 0.1 × 10^{-7}	6.5 ± 0.6
	Ca(II)[b]	2.8 ± 0.1 × 10^{-7}	4.6 ± 0.3
	Sr(II)[b]	3.4 ± 0.2 × 10^{-7}	2.3 ± 0.2
	Ba(II)[b]	3.8 ± 0.1 × 10^{-7}	6.1 ± 0.3
Fab of 5B2	metal-free	8.0 ± 0.2 × 10^{-6}	4.5 ± 0.4
	Ca(II)[b]	8.9 ± 0.2 × 10^{-6}	2.7 ± 0.2
	Sr(II)[b]	1.1 ± 0.1 × 10^{-5}	3.0 ± 0.1
	Ba(II)[b]	1.1 ± 0.1 × 10^{-5}	2.6 ± 0.2

[a] Values for $K_{0.5}$ and the Hill coefficient are shown with their 95% confidence intervals. Each pair of values represents the results of duplicate binding studies that utilized 12 different concentrations of soluble ligand. [b] The concentration of each alkaline earth, when present, was 100 mM in all experiments.

It was evident that the sigmoidal binding curves presented in Figure 4 had to arise from some property exhibited by the proteins, not from some complex interplay of equilibria among free and complexed metal ions and chelators. The large excess of calcium ions employed in both experiments, 100 mM, ensured that the two principal small molecule species in solution were free calcium ions (which themselves had no detectable ability to occupy the antigen binding sites on either the intact or the fragmented antibody) and the aminobenzyl−DTPA−Ca(II) complex. Calculations using the relevant stability constant (*22*) revealed that the concentration of metal-free aminobenzyl−DTPA never exceeded 1.0 and 50 pM in Figure 4A,B, respectively. The latter value was still only 2.5% of that of the total concentration of Fab fragment in the experiments represented in Figure 4B, so metal-free chelator was never present in concentrations that could appreciably influence the antibody or its fragment. Further, if the sigmoidal features of the binding curves in Figure 4 were due to equilibria among the small molecules alone, one would not anticipate the 30-fold difference in the values of $K_{0.5}$ observed with the intact 5B2 and its Fab fragment.

Further evidence that the sigmoidal binding curves presented in Figure 4 had to arise from some property exhibited by the proteins came from equilibrium binding studies using just the metal-free aminobenzyl−DTPA. Sigmoidal binding curves similar to those shown in Figure 4 were also obtained when intact 5B2 and its Fab fragment were incubated with metal-free aminobenzyl−DTPA in the absence of any additional metal ions (primary data not shown). Analogous fits of these data to eq 2 yielded the values for $K_{0.5}$ and n summarized in Table 2 for the two proteins and metal-free aminobenzyl−DTPA.

Analogous sigmoidal binding curves were obtained when either intact 5B2 or its Fab fragment was incubated with either aminobenzyl−DTPA−Sr(II) or aminobenzyl−DTPA−Ba(II) (primary data not shown). Values for $K_{0.5}$ and *n* obtained from the corresponding fits of these data to eq 2 are also summarized in Table 2.

The apparent Hill coefficients for the four sigmoidal binding curves obtained with the intact antibody varied from 2.3 to 6.5, while the values of $K_{0.5}$ obtained with each of the

three aminobenzyl−DTPA−alkaline earth complexes varied by less than 20% from that obtained with the metal-free chelator. Although the values of the apparent Hill coefficients obtained with the Fab were generally less than the corresponding values obtained using intact 5B2, they nonetheless ranged from 2.6 to 4.5, values considerably greater than the value of one anticipated for the monovalent Fab. Like the intact 5B2, the values of $K_{0.5}$ obtained with the Fab and each of the three aminobenzyl−DTPA−alkaline earth complexes varied by less than 30% from that obtained with the metal-free chelator, although the concentration of soluble ligand required to achieve half-maximal saturation with the Fab was approximately 30-fold higher than that required with the intact 5B2.

While strong homotropic positive cooperativity was observed with aminobenzyl−DTPA in the presence of each of the three alkaline earth metals, it should be noted that the concentrations that corresponded to half-maximal binding observed with either intact 5B2 or its Fab did not vary significantly among the metal-free chelator and its alkaline earth complexes. Similarly, the equilibrium dissociation constants obtained with 5B2 and selected alkaline earth complexes of DTPA and CHX−DTPA were little different from those obtained with the corresponding metal-free chelators (Table 1). If the relatively weak associations of DTPA and its derivatives with the individual alkaline earth metals are assumed to be in rapid equilibrium relative to the interactions with the protein, then there is no conclusive evidence that chelator−alkaline earth complexes actually bind to 5B2; all of the relevant observations reported herein could be accommodated by a model where only the metal-free chelator in rapid equilibrium with the corresponding alkaline earth complex was capable of binding to the antibody.

Heterotrophic Positive Cooperativity. Equilibrium binding studies conducted with 5B2, aminobenzyl−DTPA, and ionic lead provided evidence for heterotropic positive cooperativity when it was observed that the metal-free chelator promoted the binding of the chelator−Pb(II) complex to the antibody. The data shown in Figure 5A,B were obtained when intact 5B2 was incubated with limiting chelator in the presence of excess Pb(II) and with limiting Pb(II) in the presence of excess chelator, respectively. The concentration of excess Pb(II) employed in the binding experiments represented in Figure 5A, 100 μM, was sufficient to ensure that the limiting aminobenzyl−DTPA was present as the corresponding complex with Pb(II); based on the relevant stability constant (*22*) the concentration of metal-free aminobenzyl−DTPA in these experiments could not have exceeded 1.0 fM. In the absence of the chelator, 100 μM Pb(II) had no effect on the binding of soluble 5B2 to the immobilized capture reagent. Similarly, the concentration of excess aminobenzyl−DTPA employed in the binding experiments represented in Figure 5B, 200 nM, was sufficient to ensure that the limiting Pb(II) was present as the corresponding complex with the chelator; in these experiments, the concentration of chelator-free Pb(II) could not have exceeded 0.5 pM, a value well below that of the intact antibody present in the experiment (0.53 nM). However, since the metal-free chelator was also an inhibitory ligand for the antibody (see above), care was taken to choose a constant concentration of excess aminobenzyl−DTPA for these studies that only inhibited the binding of the intact 5B2 to the immobilized capture reagent by roughly 10% (corresponding to the beginning of the steep portion of the sigmoidal binding curve for the metal-free chelator to the antibody, data not shown). In either case, parameters for the hyperbolic curves drawn through the data points in Figure 5A,B were obtained from nonlinear regression fits of the data to eq 1. It was evident that the presence of excess metal-free aminobenzyl−DTPA increased the affinity of the intact 5B2 for aminobenzyl−DTPA−Pb(II) by about 6.6-fold.

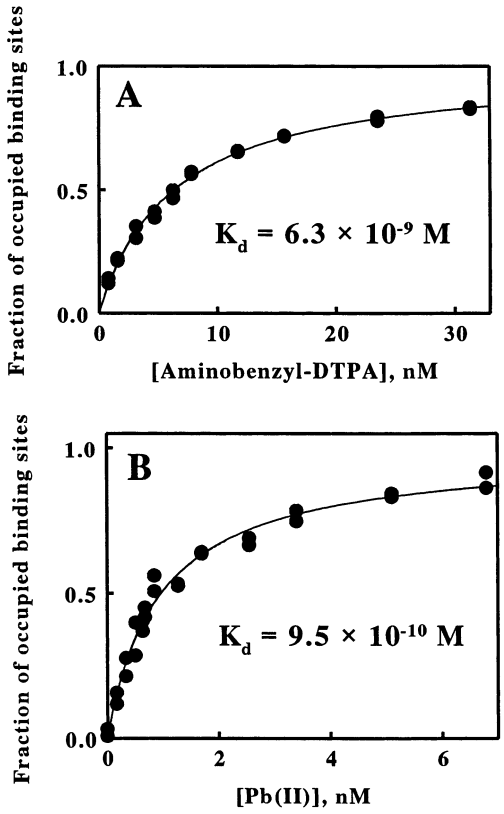

FIGURE 5: Heterotropic positive cooperativity in the binding of aminobenzyl−DTPA and its Pb(II) complex to intact 5B2. (A) Concentration dependence of the binding of aminobenzyl−DTPA to 5B2 in the presence of 100 μM Pb(II). (B) Concentration dependence of the binding of Pb(II) to 5B2 in the presence of 200 nM aminobenzyl−DTPA. Each determination was performed in duplicate. The hyperbolic curves drawn through the data points were generated using eq 1 in the text and values for the corresponding equilibrium dissociation constants (K_d) as shown in figure and in Table 3.

Similar results were obtained when the experiments described above were conducted on intact 5B2 with In(III) as a substitute for Pb(II); the results are summarized in Table 3. When 5B2 was incubated with limiting concentrations of aminobenzyl−DTPA in the presence of excess In(III), the resulting hyperbolic binding curve yielded an apparent equilibrium dissociation constant of 7.9×10^{-8} M for the binding of aminobenzyl−DTPA−In(III) to intact 5B2 (primary data not shown). The converse experiment, incubation of intact 5B2 with limiting concentrations of In(III) in the presence of 200 nM aminobenzyl−DTPA, produced a hyperbolic binding curve with an apparent equilibrium dissociation constant of 1.2×10^{-8} M. Even though the In(III) complex of aminobenzyl−DTPA bound with approximately 11-fold lower affinity to intact 5B2 than did the corresponding Pb(II) complex, the metal-free chelator appeared to promote the binding of either of the metal−chelator

Table 3: Heterotropic Positive Cooperativity in the Binding of the Pb(II) and In(III) Complexes of Aminobenzyl-DTPA with Intact 5B2 and Its Fab Fragment

protein	varied, limiting ligand[a]	constant, excess ligand[a]	apparent K_d[b],M
intact 5B2	aminobenzyl-DTPA	Pb(II)[c]	$6.3 \pm 0.3 \times 10^{-9}$
	Pb(II)	aminobenzyl-DTPA[d]	$9.5 \pm 0.7 \times 10^{-10}$
	aminobenzyl-DTPA	In(III)[e]	$7.9 \pm 0.5 \times 10^{-8}$
	In(III)	aminobenzyl-DTPA[d]	$1.2 \pm 0.1 \times 10^{-8}$
Fab of 5B2	aminobenzyl-DTPA	Pb(II)[c]	$1.8 \pm 0.1 \times 10^{-7}$
	Pb(II)	aminobenzyl-DTPA[f]	$3.3 \pm 0.2 \times 10^{-8}$
	aminobenzyl-DTPA	In(III)[e]	$2.2 \pm 0.1 \times 10^{-7}$
	In(III)	aminobenzyl-DTPA[f]	$5.5 \pm 0.3 \times 10^{-8}$

[a] Each binding experiment was conducted in the presence of an excess, constant concentration of the ligand indicated. [b] Each value represents the results of duplicate binding studies that utilized 12 different concentrations of the varied ligand. [c] [Pb(II)] = 100 μM. [d] [aminobenzyl-DTPA] = 200 nM. [e] [In(III)] = 2.5 μM. [f] [aminobenzyl-DTPA] = 2.0 μM.

complexes to the antibody to about the same extent, 6.6-fold.

Further evidence for heterotropic positive cooperativity was obtained when analogous binding studies were conducted with the Fab fragment of 5B2; the results are also summarized in Table 3. The binding of aminobenzyl−DTPA−Pb(II) to the Fab in the presence of excess Pb(II) or excess metal-free aminobenzyl−DTPA produced binding curves characterized by equilibrium dissociation constants of 1.8×10^{-7} and 3.3×10^{-8} M, respectively. Similarly, the binding of aminobenzyl−DTPA−In(III) to the Fab in the presence of excess In(III) or excess metal-free aminobenzyl−DTPA produced binding curves characterized by equilibrium dissociation constants of 2.2×10^{-7} and 5.5×10^{-8} M, respectively. Even though the Fab exhibited lower affinity and specificity for the complexes of aminobenzyl−DTPA with Pb(II) and In(III) than did the intact 5B2, the Fab nonetheless showed the same metal-free chelator-dependent stimulation of the binding of each metal−chelator complex to the protein.

Homotropic Negative Cooperativity. When equilibrium binding studies were conducted with 5B2, aminobenzyl−DTPA, and either Hg(II) or Cd(II), the resulting binding curves indicated a high degree of homotropic negative cooperativity in the interactions of the metal−chelator complex with the antibody. The equilibrium binding data shown in Figure 6A were obtained when intact 5B2 was incubated with limiting concentrations of aminobenzyl−DTPA in the presence of 50 μM Hg(II). Control experiments indicated that 50 μM Hg(II) had no apparent effect on the interaction of the soluble 5B2 with the immobilized capture reagent used to quantify the extent of binding in solution. It is clear from the data in Figure 6A that the affinity of intact 5B2 for aminobenzyl−DTPA−Hg(II) appeared to decrease as the fractional occupancy of the antibody's binding sites increased. The parameters for the biphasic curve drawn through the data points in Figure 6A were obtained from a nonlinear regression fit of the data to the following equation (*27*, *28*):

$$\text{fraction of occupied binding sites} = \frac{\beta K_1[\mathrm{L}] + [\mathrm{L}]^2}{\beta K_1^{\,2} = 2\beta K_1[\mathrm{L}] + [\mathrm{L}]^2} \quad (3)$$

where K_1 is the apparent equilibrium dissociation constant for binding of the first antigen to the antibody with both binding sites unoccupied, and β, a measure of the degree of homotrophic negative cooperativity, is equal to K_2/K_1, where K_2 is the apparent equilibrium dissociation constant for binding of the second antigen to the antibody with one occupied binding site. Values of 3.1×10^{-7} M and 11 for K_1 and β, respectively, produced the best fit of the regression line to the data in Figure 6A. A similar biphasic binding curve was obtained when 500 μM Cd(II) was substituted for Hg(II) (primary data not shown). The characteristics of the biphasic curves obtained with both metal−chelator complexes are summarized in Table 4. The values of the high and low affinity dissociation constants obtained for the binding of aminobenzyl−DTPA−Cd(II) to the intact 5B2

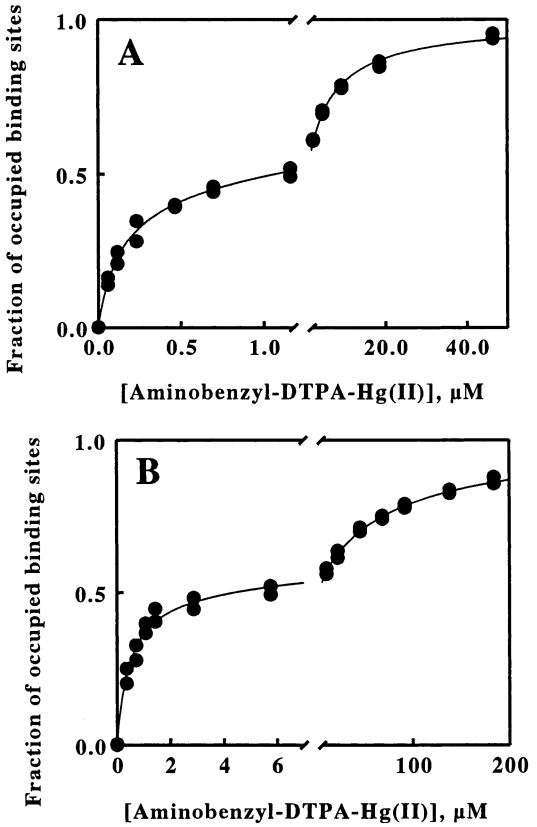

FIGURE 6: Homotropic negative cooperativity in the binding of aminobenzyl−DTPA−Hg(II) to intact 5B2 (A) and its Fab fragment (B). Aminobenzyl−DTPA at the concentrations shown on the x-axes was varied while holding the concentration of Hg(II) at 50 and 200 μM in experiments A and B, respectively. Each determination was performed in duplicate. The biphasic curves drawn through the data points were generated using eq 3 in the text and the values for the relevant constants shown in Table 4.

Table 4: Homotropic Negative Cooperativity in the Binding of the Hg(II) and Cd(II) Complexes of Aminobenzyl-DTPA with Intact 5B2 and Its Fab Fragment

protein	metal ion complexed with aminobenzyl-DTPA[a]	apparent K_1 of first phase[b], M	value of β[b]
intact 5B2	Hg(II)[c]	$3.1 \pm 0.3 \times 10^{-7}$	11 ± 1
	Cd(II)[d]	$5.3 \pm 0.6 \times 10^{-7}$	10 ± 1
Fab of 5B2	Hg(II)[e]	$8.1 \pm 0.9 \times 10^{-7}$	41 ± 3
	Cd(II)[d]	$4.1 \pm 0.7 \times 10^{-7}$	19 ± 3

[a] Each binding experiment was conducted in the presence of an excess concentration of the metal ion. [b] Values for K_1 and β were obtained from nonlinear regression analyses of the data in each set to eq 3 in the text. Each set of two values represents the results of duplicate binding studies that utilized from 12 to 17 different concentrations of the limiting ligand, the aminobenzyl-DTPA. [c] [Hg(II)] = 50 μM. [d] [Cd(II)] = 500 μM. [e] [Hg(II)] = 200 μM.

were approximately 1.7-fold higher than the corresponding values obtained in the presence of aminobenzyl−DTPA−Hg(II); otherwise, the characteristics of the two binding curves were the same.

Analogous results were obtained when the Fab of 5B2 was incubated with limiting concentrations of aminobenzyl−DTPA in the presence of 200 μM Hg(II). The resulting binding curve is presented in Figure 6B. The values of the apparent dissociation constants for the high and low affinity phases increased in the Fab by 2.6- and 10-fold, respectively, compared to those in the intact 5B2; otherwise, the characteristics of the two curves were the same. The biphasic binding curve obtained when the same Fab fragment was incubated with aminobenzyl−DTPA in the presence of excess Cd(II) was very similar to the corresponding data obtained with the intact 5B2 (Table 4). Aminobenzyl−DTPA−Hg(II) produced stronger homotropic negative cooperativity with the Fab than did aminobenzyl−DTPA−Cd(II); the values of for the two phases obtained with the aminobenzyl−DTPA complexes of Hg(II) and Cd(II) were 41 and 19, respectively.

Heterotropic Negative Cooperativity. Since it is very difficult to distinguish between homotropic negative cooperativity and simple heterogeneous binding due to functional or structural differences among the antibody proteins in solution, further equilibrium binding studies were conducted to determine whether heterotropic negative cooperativity was exhibited by 5B2 or its Fab. The results of these experiments performed with the Fab are shown in Figure 7. Figure 7A shows the binding curves for additional aminobenzyl−DTPA−Hg(II) after the available binding sites on the Fab were half-saturated with either aminobenzyl−DTPA−Hg(II) or aminobenzyl−DTPA−Cd(II). If the apparent homotropic negative cooperativity described above were simply the result of heterogeneity in the population of Fab fragments, then one would expect the two low affinity binding curves in Figure 7A to be identical, since the identity of the ligand used to fill the high affinity sites would have no influence on the behavior of the independent low affinity sites. Instead, the identity of the ligand used to fill the high affinity sites on the Fab had a clear influence on the apparent dissociation constant of the low affinity interaction between the remaining binding sites and the soluble aminobenzyl−DTPA−Hg(II) complex. The affinity of the Fab for additional aminobenzyl−DTPA−Hg(II) was higher when aminobenzyl−DTPA−Cd(II) was used to half-saturate the Fab rather than the corresponding complex with Hg(II).

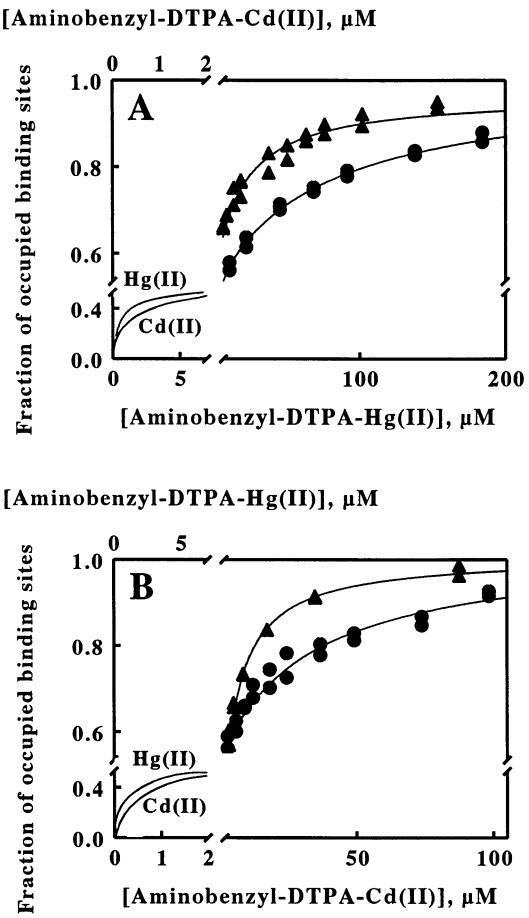

FIGURE 7: Heterotropic negative cooperativity in the binding of the aminobenzyl−DTPA complexes of Hg(II) (A) and Cd(II) (B) to the Fab fragment of 5B2. (A) Binding of additional aminobenzyl−DTPA−Hg(II) in the presence of 5.0 μM aminobenzyl−DTPA−Hg(II) (circles) or 2.0 μM Cd(II) (triangles). (B) Binding of additional aminobenzyl−DTPA−Cd(II) in the presence of 5.0 μM aminobenzyl−DTPA−Hg(II) (circles) or 2.0 μM Cd(II) (triangles). Each determination was performed in duplicate. The biphasic curves were generated as described in the legend to Figure 6. The experimental data points were omitted from the high affinity portions of the curves in both panels for clarity of presentation. The hyperbolic curves drawn through the low affinity binding data determined with aminobenzyl−DTPA−Hg(II) in the presence of aminobenzyl−DTPA−Cd(II) in A or with aminobenzyl−DTPA−Cd(II) in the presence of aminobenzyl−DTPA−Hg(II) in B were generated using values for the corresponding equilibrium dissociation constants of 17 and 32 μM, respectively.

The same conclusions were drawn when the low affinity ligand was aminobenzyl−DTPA−Cd(II), as illustrated in Figure 7B. Figure 7B shows the binding curves for additional aminobenzyl−DTPA−Cd(II) after the available binding sites on the Fab were half-saturated with either the Cd(II) or Hg(II) complexes of aminobenzyl−DTPA. Once again, the identity of the ligand used to fill the high affinity sites on the Fab had a clear influence on the apparent dissociation constant of the low affinity interaction between the remaining binding sites and the soluble aminobenzyl−DTPA−Cd(II) complex. The affinity of the Fab for additional aminobenzyl−DTPA−Cd(II) was also higher when aminobenzyl−DTPA−Cd(II) was used to half-saturate the Fab rather than the corresponding complex with Hg(II). Both the homotropic and the

heterotropic results were consistent, in that half-saturation with the Hg(II) complex exerted a stronger negative influence on the subsequent Fab binding reactions than did half-saturation with the Cd(II) complex. This would not occur in simple heterogeneous binding.

The intact 5B2 was subjected to N-terminal sequence analysis to provide ancillary structural data on the degree of homogeneity of the purified antibody preparation. The first 25 residues of the heavy chain, EVQLQQSGAELLKPGAS-VKLSCTTS, yielded single peaks with very strong, unequivocal signals (with the exception of the conserved C, residue number 22); a heterogeneous protein would not have provided such data. A blocked amino terminal in the light chain precluded sequencing of this subunit.

DISCUSSION

An immediate concern in the interpretation of the complex binding behavior described above is the fact that the soluble antigen, a chelator−metal complex, can undergo dissociation to yield the corresponding free metal ion and free chelator, either or both of which can also bind to the antigen site on the antibody. This situation is analogous to many studies conducted over the last 30-plus years on the mechanism of action of enzymes that transform polyvalent anions (like ATP or ADP) and require divalent cations (like Mg(II) or Mn(II)) for activity (*29*, *30*). Further complications arise in these latter studies when (i) more than one metal-complexed substrate is involved in the reaction and each substrate has a different affinity for the metal ion, and (ii) the equilibrium dissociation constants for the substrate−metal complexes are of the same order of magnitude as the concentrations of total substrate and metal ion employed in the study. One can reach definitive conclusions about the mechanism(s) of binding under these difficult conditions only if (i) one carefully recalculates the concentrations of each complexed and free species whenever the concentration of a single reagent is changed, and (ii) different solutions in a series of equilibrium or kinetic experiments are carefully crafted to rigorously maintain the constant concentration of one of the components, such as free, uncomplexed metal ion (*29*, *30*). This was precisely the approach employed previously by our laboratories (*15*), where the apparent positive cooperativity observed with antibody 2C12 in the presence of CHX−DTPA and Pb(II) was traced to the bimolecular association of equal concentrations of the chelator and the Pb(II) to form the complex actually recognized by the antibody, not to some binding-dependent conformation change in the antibody.

In the present case, the extraordinary effects described above must be attributed to the binding properties of the antibody itself, not to some complex interplay of equilibria among free and complexed metal ions and chelators. The combination of the relatively high affinity of the chelator for the metal ion coupled with the relatively low affinity of the 5B2 antibody and its Fab fragment for the chelator or chelator−metal ion complex served to greatly simplify the experimental design. All of the equilibrium binding studies presented herein were conducted under conditions in which there were only two small ligand reagents present in concentrations equal to or in excess of that of the antibody: the chelator−metal ion complex of choice; and an excess of either the metal-free chelator or the chelator-free metal. Control experiments indicated that chelator-free metal ions (when the total chelator concentration was limiting) or metal-free chelators (when the total concentration of metal ions was limiting) at excess high concentrations had undetectable or insignificant effects, respectively, on the direct occupation of the antigen binding site.

Any attempt to rationalize the complex binding behavior observed for 5B2 and its Fab fragment must account for both the complexity and the apparent multiplicity of binding of aminobenzyl−DTPA and its various metal ion complexes. Three general features of protein structure seem particularly favorable for the appearance of complex interligand effects such as those described herein. First, proteins are polyelectrolytes, and their properties are critically dependent upon the ionic strength and specific ion composition of the solvent, particularly the concentration of hydrogen ions. Proteins cannot be found in solution free from counterions. Aminobenzyl−DTPA and its metal ion complexes comprise highly charged, hydrophilic species that, in addition to interacting with the antigen binding site in this case, can also serve as counterions at a variety of polar sites on the surface of the globular antibody exposed to solvent. These considerations could readily account for the binding of multiple highly charged DTPA species to antibody 5B2 or its Fab fragment.

Second, the compact globular structure present in antibodies provides a core region of relatively low polarizability out of contact with the solvent. Binding of two or more highly charged ions will result in much stronger electrostatic interactions through the core of the protein than when the same ions are free in solution in a highly polar solvent like water. Similar remarks apply to the interactions between a bound, charged ligand and charged or polarizable groups on the protein involved in the binding of a second charged (or even uncharged) ligand. It is evident that the binding of multiple charged ligands to a globular protein could result in a very complex pattern of interactions among the bound ligands and their respective sites on the protein.

Third, proteins maintain secondary, tertiary, and quaternary structure by virtue of a large number of independent, or nearly independent, short-range small energy interactions. As a result, the addition of a bound ligand must always produce some changes in the energetic balance of its immediate surroundings. Consequently, one could argue that we never deal with the binding of a single charged ligand to a protein, but that simultaneous, interacting equilibria are the rule when proteins and charged ligands are considered. Indeed, recent structural studies on Fab fragments directed against a variety of charged antigens have revealed that significant conformation changes can occur within the Fab as a consequence of antigen binding (*31*−*34*). Similarly, other studies using intact monoclonal antibodies directed against fluorescein and lysozyme have revealed that secondary interactions external to the antibody active site can affect ligand binding efficiency, protein dynamics, and variable domain conformation (*35*−*41*).

Since many cases of polyvalent, multiple ligand binding to proteins are known, conditions for the appearance of effects such as those reported here must be present in many compact globular proteins under the right circumstances. The observations reported over a quarter century ago by Weber and associates (*27*, *42*) in their elegant studies on the binding of multiple organic anions by BSA are a good example. The

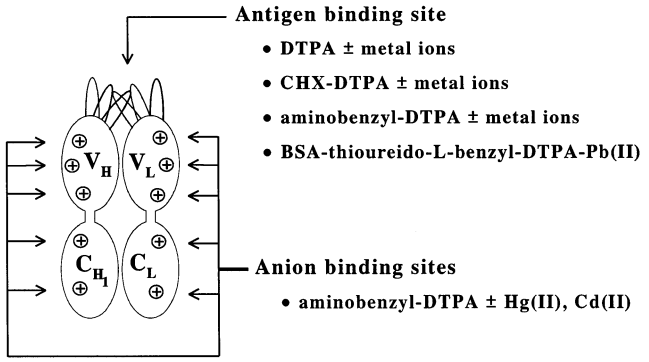

FIGURE 8: Illustrative model for the Fab fragment of antibody 5B2. This model depicts the proposed multiple anion binding sites on the surface of the protein.

binding of 1-anilinonaphthalene-8-sulfonate (ANS) by monomeric BSA was studied by equilibrium dialysis and fluorescence enhancement measurements in the presence and absence 3,5-dihydroxybenzoate (DHB). Binding of the DHB to the multiple ($\geq$ 11) low affinity anion binding sites on surface of the BSA induced positive cooperativity among the molecules of ANS that bound to the four high affinity sites, while concomitantly lowering the overall affinity of BSA for ANS. The same effects were not observed when inorganic anions were substituted for DHB, so even the low affinity sites on the BSA exercised some degree of specificity. We hypothesize that the complex anion binding properties exhibited by 5B2 arise from the same phenomenon, the binding of aminobenzyl−DTPA and its derivatives to not only the antigen binding site, but also to multiple charged sites on the surface of the compact, folded immunoglobulin. Further, we hypothesize that the bound ligands interact in a complicated fashion through the apolar core of the antibody.

The simple illustration presented in Figure 8 summarizes the arguments developed above to rationalize the remarkable binding properties of 5B2 and its Fab. The Fab fragment of the antibody is depicted by two pairs of two linked ovals, each oval representing a domain in the constant or variable portion of the light or heavy chain, as shown. The traditional antigen binding site is depicted by the short loops extending from the variable portions of the light and heavy chains. As indicated in the drawing, the antigen binding site should be capable of binding all of the soluble ligands investigated herein. A number of potential anion binding sites are depicted on the external surface of the Fab that are spatially separated from the antigen binding site. The location and number of anion binding sites shown in the drawing are arbitrary; the illustration is simply meant to convey that many organic anion binding sites are possible on the Fab (recall that BSA possesses $\geq$ 11 such sites). Charged organic ligands bound to the external sites are hypothesized to interact with each other and the antigen binding site through the apolar core of the proteins to create the complex binding characteristics reported herein. Only the Fab fragment of 5B2 is depicted in Figure 8 because the Fab exhibited the same rich variety of allosteric binding behavior as did the intact antibody.

In summary, antibodies are proteins. Individual proteins can exhibit a wide variety of allosteric binding phenomena in the presence of appropriate binding partners and solution conditions. Therefore, it is not particularly surprising that antibody 5B2 displayed the complex allosteric binding characteristics described above. What is perhaps more surprising is that analogous allosteric binding behavior has not been widely reported for other antibodies that bind highly charged ligands.

REFERENCES

1. Carayon, P., and Carella, C. (1974) Evidence for positive cooperativity in antigen−antibody reactions. *FEBS Lett. 40*, 13−17.
2. Mazza, M. M., and Retegui, L. A. (1989) Monoclonal antibodies to human growth hormone induce an allosteric conformational change in the antigen. *Immunology 67*, 148−153.
3. Aguilar, R. C., Retegui, L. A., Postel-Vinay, M. C., and Roguin, L. P. (1994) Allosteric effects of monoclonal antibodies on human growth hormone. *Mol. Cell Biochem. 136*, 35−42.
4. Reineke, U., Schneider-Mergener, J., Glaser, R. W., Stigler, R. D., Seifert, M., Volk, H. D., and Sabat, R. (1999) A synthetic mimic of a discontinuous binding site on interleukin-10. *J. Mol. Recognit. 12*, 242−248.
5. Weber-Bornhauser, S., Eggenberger, J., Jelesarov, I., Bernard, A., Berger, C., and Bosshard, H. R. (1998) Thermodynamics and kinetics of the reaction of a single-chain antibody fragment (scFv) with the leucine zipper domain of transcription factor GCN4. *Biochemistry 37*, 13011−13020.
6. Nowakowski, A., Wang, C., Powers, D., Amersdorfer, P., Montgomery, V., Sheridan, R., Blake, R., Smith, L., and Marks, J. D. (2002) Potent neutralization of botulinum neurotoxin by recombinant oligoclonal antibody. *Proc. Natl. Acad. Sci. U.S.A. 99*, 11346−11350.
7. van Erp. R., Gribnau, T. C., van Sommeren, A. P., and Bloemers, H. P. (1991) Affinity of monoclonal antibodies. Interpretation of the positive cooperative nature of anti-hCG/hCG interactions. *J. Immunol. Met. 140*, 235−241.
8. Holmes, N. J., and Parham, P. (1983) Enhancement of monoclonal antibodies against HLA-A2 is due to antibody bivalency. *J. Biol. Chem. 258*, 1580−1586.
9. Wellerson, R., and Kaplan, P. (1986) Enhanced binding activity observed between anti-carcinoembryonic monoclonal antibodies. *Hybridoma 5*, 199−213.
10. Ehrlich, P. H., and Moyle, W. R. (1983) Cooperative immunoassays: ultrasensitive assays with mixed monoclonal antibodies. *Science 221*, 279−281.
11. Moyle, W. R., Anderson, D. M., and Ehrlich, P. H. (1983) A circular antibody−antigen complex is responsible for increased affinity shown by mixtures of monoclonal antibodies to human chorionic gonadotropin. *J. Immunol. 131*, 1900−1905.
12. Ehrlich, P. H., and Moyle, W. R. (1984) Specificity considerations in cooperative immunoassays. *Clin. Chem. 30*, 1523−1532.
13. Moyle, W. R., Lin, C., Corson, R. L., and Ehrlich, P. H. (1983) Quantitative explanation for increased affinity shown by mixtures of monoclonal antibodies: importance of a circular complex. *Mol. Immunol. 20*, 439−452.
14. Blake, D. A., Chakrabarti, P., Khosraviani, M., Hatcher, F. M., Westhoff, C. M., Goebel, P., Wylie, D. E., and Blake, R. C., II (1996) Metal binding properties of a monoclonal antibody directed toward metal-chelate complexes. *J. Biol. Chem. 271*, 27677−85.
15. Khosraviani, M., Blake, R. C., II, Pavlov, A. R., Lorbach, S. C., Yu, H., Delehanty, J. B., Brechbiel, M. W., and Blake, D. A. (2000) Binding properties of a monoclonal antibody directed toward lead-chelate complexes. *Bioconj. Chem. 11*, 267−77.
16. Blake, D. A., Pavlov, A. R., Yu. H., Khosraviani, M., Ensley, H. E., and Blake, R. C. II (2001) Antibodies and antibody-based assays for hexavalent uranium. *Anal. Chim. Acta 444*, 3−11.
17. Jones, R. M., Yu, H., Delehanty, J. B., and Blake, D. A. (2002) Monoclonal antibodies that recognize minimal differences in the three- dimensional structures of metal-chelate complexes. *Bioconj. Chem. 13*, 408−415.
18. Brechbiel, M., Gansow, O. A., Atcher, R. A., Schlom, J., Esteban, J., Simpson, D. E., and Colcher, D. (1986) Synthesis of 1-(*p*-isocyanotobenzyl) derivatives of DTPA and EDTA: Antibody labeling and tumor-imaging studies. *J. Inorg. Chem. 2*, 2772−2781.
19. Cayot, P., and Tainturier, G. (1997) The quantification of protein amino groups by the trinitrobenzenesulfonic acid method: a reexamination. *Anal. Biochem. 249*, 184−200.

20. Chakrabarti, P., Hatcher, F. M., Blake, R. C., II, Ladd, P. A., and Blake, D. A. (1994) Enzyme immunoassay to determine heavy metals using antibodies to specific metal-EDTA complexes: optimization and validation of an immunoassay for soluble indium. *Anal. Biochem. 21*, 70−5.
21. Livingston, D. M. (1974) Immunoaffinity chromatography of proteins. *Met. Enzymol. XXXIV*, 723−731.
22. Martell, A. E., and Smith, R. M. (1998) *NIST Critically Selected Stability Constants of Metal Complexes*, version 5.0, NIST Standard Reference Data, National Institutes of Standards and Technology.
23. McMurry, T. J., Pippin, C. G., Wu, C., Deal, K. A., Brechbiel, M. W., Mirzadeh, S., and Gansow, O. A. (1998) Solution equilibria, acid dissociation. and serum stability studies of yttrium(III) complexes of C-functionalised diethylenetriamine-*N*,*N*′,*N*″-pentaacetic acid ligands. *J. Med. Chem. 41*, 3546−3549.
24. Kennedy, J. H. (1984) in *Analytical Chemistry: Principles*, pp 281−303, Harcourt Brace Jovanovich, New York.
25. Blake, R. C., II, Pavlov, A. R., and Blake, D. A. (1999) Automated kinetic exclusion assays to quantify protein binding interactions in homogeneous solution. *Anal. Biochem. 272*, 123−34.
26. Blake, D. A., Khosraviani, M., Pavlov, A. R., and Blake, R. C., II. (1997) in *Immunochemical Technology for Environmental Applications* (Aga, D. S., and Thurman, E. M., Eds.) American Chemical Society, Washington, DC.
27. Weber, G. (1975) Energetics of ligand binding to proteins. *Adv. Protein. Chem. 29*, 1−83.
28. Weber, G. (1972) Ligand binding and internal equilibria in proteins, *Biochemistry 11*, 864−878
29. London, W. P., and Steck, T. L. (1969) Kinetics of enzyme reactions with interaction between a substrate and a (metal) modifier. *Biochemistry 8*, 1767−1779.
30. Morrison, J. F. (1979) Approaches to kinetic studies on metal-activated enzymes. *Met. Enzymol. 63*, 257−294.
31. Guddat, L. W., Shan, L., Anchin, J. M., Linthicum, D. S., and Edmundson, A. B. (1994) Local and transmitted conformational changes on complexation of an anti-sweetener Fab. *J. Mol. Biol. 236*, 247−274.
32. Stanfield, R. L., Takimoto-Kamimura, M., Rini, J. M., Profy, A. T., and Wilson, I. A. (1993) Major antigen-induced domain rearrangements in an antibody. *Structure 1*, 83−93.
33. Kodandapani, R., Veerapandian, L., Ni, C. Z., Chiou, C. K., Whittal, R. M., Kunicki, T. J., and Ely, K. R. (1998) Conformational change in an anti-integrin antibody: structure of OPG2 Fab bound to a beta 3 peptide, *Biochem. Biophys. Res. Commun. 251*, 61−66.
34. Monaco-Malbet, S., Berthet-Colominas, C., Novelli, A., Battai, N., Piga, N., Cheynet, V., Mallet, F., and Cusack, S. (2000) Mutual conformational adaptations in antigen and antibody upon complex formation between an Fab and HIV-1 capsid protein p24. *Struct. Fold Des. 8*, 1069−1077.
35. Mummert, M. E., and Voss, E. W., Jr. (1996) Effects of secondary forces on the ligand binding properties and variable domain conformations of a monoclonal anti-fluorescyl antibody. *Mol. Immunol. 33*, 1067−1077.
36. Mummert, M. E., and Voss, E. W., Jr. (1997) Effects of secondary forces on the ligand binding and conformation state of anti-fluorescein monoclonal antibody 9−40. *Biochemistry 36*, 11918−11922.
37. Mummert, M. E., and Voss, E. W., Jr. (1996) Effects of secondary forces on a high affinity monoclonal IgM anti-fluorescein antibody possessing cryoglobulin and other cross-reactive properties. *Mol. Immunol. 35*, 103−113.
38. Mummert, M. E., and Voss, E. W., Jr. (1996) Secondary force-mediated perturbations of antifluorescein monoclonal antibodies 4-4-20 and 9-40 as determined by circular dichroism, *J. Protein Chem. 17*, 237−244.
39. Benjamin, D. C., Williams, D. C., Jr., Smith-Gill, S. J., and Rule, G. S. (1992) Long-range changes in a protein antigen due to antigen−antibody interaction. *Biochemistry 31*, 9539−9545.
40. Lavoie, T. B., Drohan, W. N., and Smith-Gill, S. J. (1992) Experimental analysis by site-directed mutagenesis of somatic mutation effects on affinity and fine specificity in antibodies specific for lysozyme. *J. Immunol. 148*, 503−513.
41. Padlan, E. A., Silverton, E. W., Sheriff, S., Cohen, G. H., Smith-Gill, S. J., and Davies, D. R. (1989) Structure of an antibody−antigen complex: crystal structure of the HyHEL-10 Fab-lysozyme complex. *Proc. Natl. Acad. Sci. U.S.A. 86*, 5938−5942.
42. Kolb, D. A., and Weber, G. (1975) Cooperativity of binding of anilinonaphthalenesulfonate to serum albumin induced by a second ligand. *Biochem. 14*, 4476−4481.

BI0267339